effectively changes the layer ordering; when the chains are in the $-x + y$, $+x - y$ quadrants a type 3(b) system is obtained, and when the chains are in the $+x + y$, $-x - y$ quadrants a type 3(a) class is obtained. This rotation (based on previous results) fixes the sign of the spontaneous polarization.

Gauche conformers can also be accounted for in this construction by simply changing the all-trans conformation to ones including gauche bonds, as shown in Figure 7b. Comparing the structures 7(a) to 7(b) predicts a change in the sign of the spontaneous polarization for these two (*Sed*) homologues even when they have the same tilt orientation.

Unlike the case for the spontaneous polarization direction, a fuller understanding of the factors that influence the twist sense has still not been achieved, and therefore the root cause and mechanism of the twist in dissymmetric smectic phases remains unresolved. Finally, it is interesting to note that the same relationships which apply to smectics also operate for cholesterics. The spiral ordering in these two modifications occurs in different directions, lateral to the long axis in cholesterics and normal to the layers in tilted smectic phases. Seemingly this would support the evidence already obtained that the twist sense is not sensitive to dipolar orientational ordering.

(V) Conclusion

A hypothesis has been developed to explain the anomalous materials discovered which do not fit the spontaneous polarization direction–twist sense rules for ferroelectric liquid crystals proposed previously. This hypothesis proposes that changes in the steric tilt orientation of the molecules or conformational changes within the molecular structure are responsible for changes to the direction of the spontaneous polarization. The twist sense on the other hand was found in all these cases to be in agreement with the previous results and therefore it appears to be insensitive to orientational or conformational changes. The spontaneous polarization direction can be determined by examining the spatial orientation of the lateral component of the dipole at the chiral center relative to the tilt axis of the phase. The twist sense, however, is not sensitive to this lateral component, and therefore it is not effected by changes in its direction relative to the molecular long axis. However, it is still difficult to isolate single microscopic factors that determine the twist sense, and hence the root cause of the twist still remains an enigma. Thus, further studies of materials with different chiral groups bound to the liquid crystal core need to be made in order to substantiate these relationships and to elucidate the twist mechanism.

Acknowledgment. The authors are grateful to Dr. J. S. Patel for many useful discussions.

Registry No. II, 74109-50-5; V ($m = 3$, $n = 9$, $p = 2$), 102808-42-4; VI, 70116-35-7; VII, 90937-74-9; XI, 102808-40-2; XII, 102808-41-3; $C_7H_{15}OPhCOOPhCH{=}C(CN)COO2M4$, 90937-70-5; $C_8H_{17}OPhCOOPhCH{=}C(CN)COO2M4$, 90937-71-6; $C_{12}H_{25}PhSOCPhPhO2M4$, 102829-71-0; $C_7H_{15}OPhOCOPhO4M6$, 90937-55-6; $C_9H_{19}OPhOCOPhO4M6$, 90937-57-8.

Hydrogen on Zinc Oxide. Theory of Its Heterolytic Adsorption

Alfred B. Anderson* and Jeffrey A. Nichols†

Contribution from the Chemistry Department, Case Western Reserve University, Cleveland, Ohio 44106. *Received December 9, 1985*

Abstract: An atom superposition and electron delocalization molecular orbital study is made of the adsorption of hydrogen species on the $(10\bar{1}0)$ prism surface of zinc oxide. 4s + 4p surface states on Zn^{2+} play a role in $H^{\bullet}$ adsorption on Zn^{2+} and O^{2-} surface sites. In the former case they provide the covalent stabilization of the Zn^{2+}–$H^{\bullet}$ bond and in the latter case they are reduced, allowing a strong O^{2-}–H^{+} bond to form. Because of this, H_2 adsorbs heterolytically, yielding Zn^{2+}–H^{-} and O^{2-}–H^{+} as the products of dissociative chemisorption. Our findings, which are based on calculations on a $Zn_{14}O_{14}$ cluster model, including surface relaxation, of the $(10\bar{1}0)$ surface are used to discuss the conductivities of the polar (0001) and $(000\bar{1})$ cleavage surfaces, the former consisting of Zn^{2+} and the latter of O^{2-}. It is suggested that the conductivities which are established when $H^{\bullet}$ adsorbs on either surface are the consequences of surface and edge sites associated with step defects and the reduction of step Zn^{2+} surface face and edge states when $H^{\bullet}$ adsorbs to step face and edge O^{2-} ions, respectively. Heterolytic adsorption of H_2 does not change the insulating property of ZnO.

Zinc oxide powder catalysts have been known for 25 years from infrared spectra to adsorb molecular hydrogen heterolytically[1]

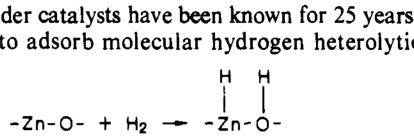

$$\text{-Zn-O-} + H_2 \rightarrow \overset{\displaystyle H}{\overset{|}{\text{-Zn}}}\text{-}\overset{\displaystyle H}{\overset{|}{\text{O}}}\text{-} \qquad (1)$$

covering 5–10% of the surface sites.[2] This rapidly reversible reaction at room temperture provides active hydrogen atoms which hydrogenate ethylene and CO to form ethane and methanol. These processes are catalytic.

Heterolytic H_2 chemisorption does not change the conductivity of ZnO, which is an insulator.[2] This also indicates the adsorption is heterolytic, with H^- bonded to Zn^{2+} and H^+ bonded to O^{2-}. A second type of IR inactive and nonconductivity inducing hydrogen adsorption, called type II, takes place slowly and irreversibly.[1-3] Type II hydrogen does not exchange easily with the reversibly adsorbed type I form. Nothing is known about the form and location of type II hydrogen though it has been speculated that it may partially penetrate into bulk octahedral sites of the wurtzite structure crystal.[3] We shall not consider it further.

Hydrogen atom adsorption at 90 K on the polar (0001) and $(000\bar{1})$ cleavage surfaces causes the surface conductivity to increase.[4,5] The (0001) surface has Zn^{2+} in its top layer and the

---

* Address inquiries to this author.

† Permanent address: Chemistry Department, Malone College, Canton, Ohio 44709.

(1) Eischens, R. P.; Pliskin, W. A.; Low, M. J. D. *J. Catal.* **1962**, *1*, 180.
(2) Kokes, R. J. *Acc. Chem. Res.* **1973**, *6*, 222 and references therein.
(3) Dent, A. L.; Kokes, R. J. *J. Phys. Chem.* **1969**, *73*, 3781.
(4) Moormann, H.; Kohl, D.; Heiland, G. *Surf. Sci.* **1979**, *80*, 261.
(5) Heiland, G.; Kunstmann, P. *Surf. Sci.* **1969**, *13*, 72.

0002-7863/86/1508-4742$01.50/0 © 1986 American Chemical Society

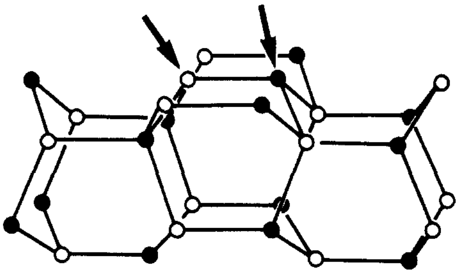

Figure 1. $Zn_{14}O_{14}$ cluster model of the $(10\bar{1}0)$ surface of ZnO. Arrows indicate well-coordinated atoms on which H adsorption is studied.

Table I. Calculated Dissociation Energies, D_0 (eV), Bond Lengths, R_e (Å), Vibrational Force Constants, k_e (mdyn/Å), and Vibrational Frequencies, ω_e (cm^{-1}), for Diatomic Molecules Using the Bulk and Surface Adapted Parameters[a]

molecule	D_0[b]	R_e	k_e	ω_e
OH^+	3.56 (5.1_4)	1.09 (1.03)	5.086 (5.41)	3018 (3113)
OH	3.58 (4.39)	1.09 (0.97)	5.086 (7.81)	3018 (3738)
OH^-	3.60 (5.47)	1.09 (0.97)	5.086 (~7.6)	3018 (~3700)
ZnH	0.88 (0.85)	1.63 (1.59)	1.974 (1.51)	1838 (1607.6)
ZnH^+	3.11 (~2.5)	1.52 (1.51)	4.208 (2.15)	2683 (1916)

[a] Experimental results in parantheses from: Huber, K. P.; Herzberg, G. *Molecular Structure IV. Constants for Diatomic Molecules*; Van Nostrand: New York, 1979. [b] These refer to the binding of H^+, H, and H^- to O and Zn.

$(000\bar{1})$ surface has O^{2-} in its top layer. It has been proposed that initial adsorption is

$$H^\bullet + O^2 \rightarrow OH^- + e^- \quad (2)$$

and the electron is promoted to a surface conduction band. Additional hydrogen atom adsorption on the prism $(10\bar{1}0)$ face, which has an equal number of Zn^{2+} and O^{2-} sites, after O^{2-} sites are reacted, would then be on zinc ions:

$$H^\bullet + Zn^+ \rightarrow (ZnH)^+ = Zn^{2+}{-}H^- \quad (3)$$

The observed blocking[6] of Zn^{2+} sites to CO at 90 K suggests that additional $H^\bullet$ is bonding to Zn^{2+}. Carbon monoxide is well-known to adsorb to Zn^{2+} sites of powder surfaces[2,7,8] and on at least four crystallographic surface planes, (0001), $(000\bar{1})$, $(10\bar{1}0)$, and $(11\bar{2}0)$.[9-11]

When $H^\bullet$ is adsorbed to (0001) ZnO, which has a Zn^{2+} surface, the conductivity slowly increases to a constant value, but on the $(000\bar{1})$ O^{2-} covered surface, hydrogen increases the conductivity rapidly to the same final value.[5] The rapid conductivity increase for the O^{2-} surface is understandable from (2), and the development of any conductivity for the Zn^{2+} covered surface indicates, it seems to us, that there must be some surface restucturing to bring O^{2-} forth. This will be discussed below further.

The adsorption of H_2 on heteronuclear surfaces occurs in numerous catalytic processes, yet the nature of adsorption, whether it is heterolytic or homolytic, is known unequivocally only for ZnO and several alkaline-earth oxides.[12] It is therefore of fundamental interest to study the mechanism of H_2 adsorption through the use of experimental and theoretical techniques. In this paper we give the results of a molecular orbital study of $H^\bullet$ adsorption on cluster models of the $(10\bar{1}0)$ surface of ZnO. From what we learn about bonding and electronic structures in this work, we will make some suggetions concerning relationships between surface restructuring and conductivity on the (0001) and $(000\bar{1})$ surfaces. Hopefully, this will stimulate the undertaking of more experimental work on the interesting unanswered questions concerning hydrogen adsorption on (0001) and $(000\bar{1})$ ZnO.

Table II. Calculated Desorption Energies, D_0 (eV), Bond Lengths, R_e (Å), Surface Atom Displacement along the Tetrahedral Direction, Δ (Å), Vibrational Frequency, ω_e (cm^{-1}), for H^+, $H^\cdot$, and H^- Adsorption on Sites of the $Zn_{14}O_{14}$ Cluster Model of the ZnO $(10\bar{1}0)$ Surface Indicated by arrows in Figure 1[a]

bond	D_0	R_e	Δ	k_e	ω_e[b]	(exptl)[c]
$Zn^{2+}{-}H^-$	0.95	1.57	0.25	3.161	2325	1709
$Zn^{2+}{-}H^\cdot$	1.43	1.57	0.25	3.158	2324	
$O^{2-}{-}H^+$	4.56	1.06	0.0	6.296	3357	3489
$O^{2-}{-}H^\cdot$	1.10[d] 2.29[e]	1.06	0.0	6.296	3357	

[a] As discussed in ref 11, on the clean surface Zn^{2+} relaxes inward along the tetrahedral direction by 0.4 Å and O^{2-} relaxes similarly by 0.15 Å. [b] Calculated from k_e with use of a diatomic approximation with no coupling to surface. [c] Reference 1. [d] Adsorption energy when the $H^\cdot$ electron is promoted to a surface state orbital on zinc which is in a bulk-like unrelaxed position. [e] Adsorption energy when the $H^\cdot$ electron is promoted to an edge state orbital on zinc which is in a bulk-like unrelaxed position. These states exist on step edges on the (0001) surface and are taken from the $Zn_{14}O_{14}$ cluster model of the $(10\bar{1}0)$ surface shown in Figure 1.

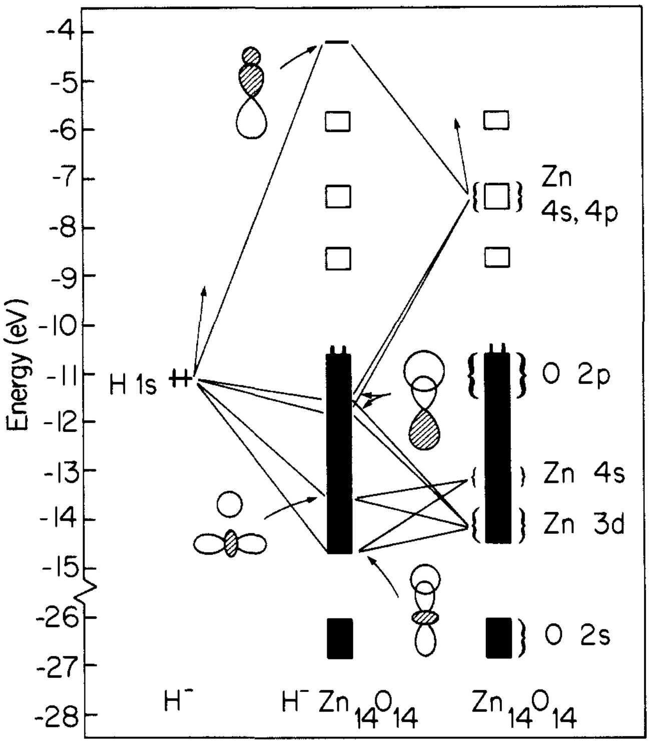

Figure 2. Energy level correlation diagram for H^- bonding to a well-coordinated surface Zn^{2+} from Figure 1. The Zn 4s + 4p empty surface state band is for unrelaxed surface; edge state bands are above and below this band.

We employ the atom superposition and electron delocalization molecular orbital method,[13] as used in our recent study of CO adsorption on (0001), $(000\bar{1})$, and $(10\bar{1}0)$ surfaces of ZnO.[11] Zn and O atomic parameters are taken from that study. Hydrogen atom parameters used here are 11.1 eV for the 1s ionization potential and 1.2 au for the corresponding orbital exponent. Our $Zn_{14}O_{14}$ cluster model of the $(10\bar{1}0)$ ZnO surface is shown in Figure 1. A pair of adjacent Zn^{2+} and O^{2-} ions shown by arrows

---

(6) D'Amico, K. L.; McClellan, M. R.; Sayers, M. J.; Gay, R. R.; McFeely, F. R.; Solomon, E. I. *J. Vac. Sci. Technol.* **1979**, *17*, 1080.

(7) Boccuzzi, F.; Garrone, E.; Zechina, A.; Bossi, A.; Camia, M. *J. Catal.* **1978**, *51*, 160.

(8) Waddams, A. L. *Chemicals in Petroleum*, 3rd ed.; Wiley: New York, 1973.

(9) Gay, R. R.; Nodine, M. H.; Henrich, V. E.; Zieger, H. J.; Solomon, E. I. *J. Am. Chem. Soc.* **1980**, *102*, 6752.

(10) D'Amico, K. L.; McFeely, F. R.; Solomon, E. I. *J. Am. Chem. Soc.* **1983**, *105*, 6380.

(11) Anderson, A. B.; Nichols, J. A. *J. Am. Chem. Soc.* **1986**, *108*, 1385.

(12) Ito, T.; Kuramoto, M.; Yoshioka, M.; Tokuda, T. *J. Phys. Chem.* **1983**, *87*, 4411.

(13) Anderson, A. B. *J. Chem. Phys.* **1975**, *62*, 1187.

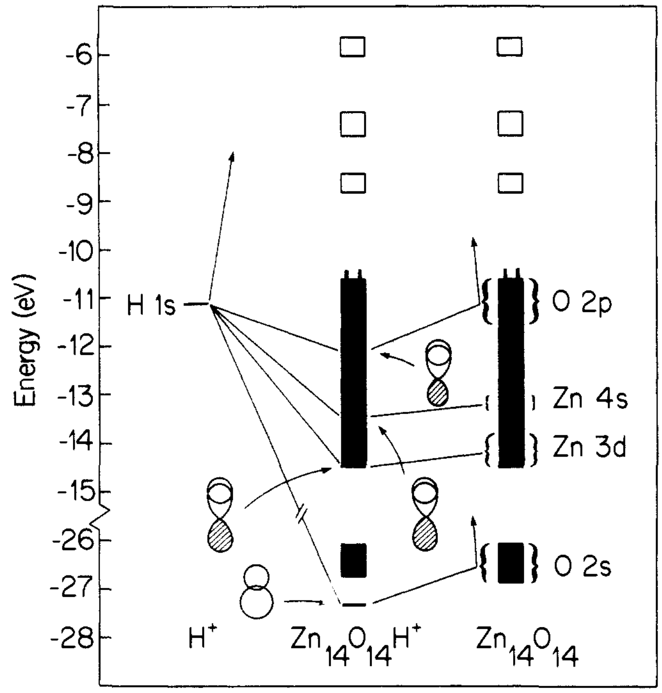

Figure 3. Energy level correlation diagram for H^+ bonding to a well-coordinated surface O^{2-} from Figure 1.

in the top center is coordinated to all nearest neighbors which themselves are coordinated to their nearest neighbors. It is on these ions that we study H• binding.

Some calculated diatomic propeties obtained with use of these surface adapted parameters are compared with experiment in Table I. Bond strengths between O and H^+, H•, and H^- are underestimated by 31, 18, and 34% respectively; those between Zn and H and H^+ are overestimated by 4 and ~24%. Thus it is possible that our calculations will overestimate the bond strengths between surface Zn^{2+} and hydrogen species, and this may be important to our surface analysis.

Heterolytic vs. Homolytic H_2 Adsorption

The H binding energies in Table II indicate clearly that heterolytic H_2 adsorption is most stable. The O^{2-}–H^+ + Zn^{2+}–H^- surface bond strengths add 5.51 eV compared to 2.86 eV for two Zn^{2+}–H• bonds and 2.20 eV for two O^{2-}–H• bonds. With estimated bond strength corrections homolytic adsorption on O^{2-} becomes favored over that on Zn^{2+}. The interaction energy of two hydrogen species on adjacent Zn and O sites is slightly repulsive by 0.06 eV, and relaxations the same as for separate hydrogen species are predicted.

The bonding of H species to the surface sites may be understood from the electronic structure and orbital correlation diagrams of Figures 2 and 3. These energy levels do not show the relaxation shifts which affect electronic structure measurements in ionization spectroscopy. The electronic structure of the zinc oxide surfaces was explained in detail in our previous paper.[11] The important features are the filled O 2p, Zn 4s, and Zn 3d bands and the empty Zn 4s, 4p surface state band, all labeled in Figure 2. Unlike oxides of transition metals from the groups to the left of zinc, the filled O 2p band lies above the zinc 3d band, and its orbitals are antibonding rather than bonding to the zinc orbitals. Below it is a Zn 4s band, which is made up of Zn 4s + O 2p bonding orbitals. Next comes the Zn 3d band whose orbitals have small bonding contributions from the oxygen 2p orbitals. The lowest band, oxygen 2s, has some small mixing of Zn 4s and 4p orbitals in a bonding way. All of the bulk and surface state contributions to these bands are indicated by curley brackets in Figure 2. The states between the O 2p and Zn 4s and Zn 4s and Zn 3d bands are edge states due to the edge atoms of the cluster model which are coordinated to only two neighbors. An empty Zn 4s + 4p surface state band is also shown in Figure 2. This is made of linear combinations dangling s–p hybrid orbitals centered on the surface Zn^{2+} ions and directed away from the surface along the tetrahedral direction. These orbitals are what allow CO to chemisorb by donation form its filled 5σ orbital into it, as shown in our earlier study.[11] Empty bands adjacent to the surface state bands are edge state bands which would be absent on an infinitely extended surface, but are present at steps on (0001) and (000$\bar{1}$) surfaces discussed below.

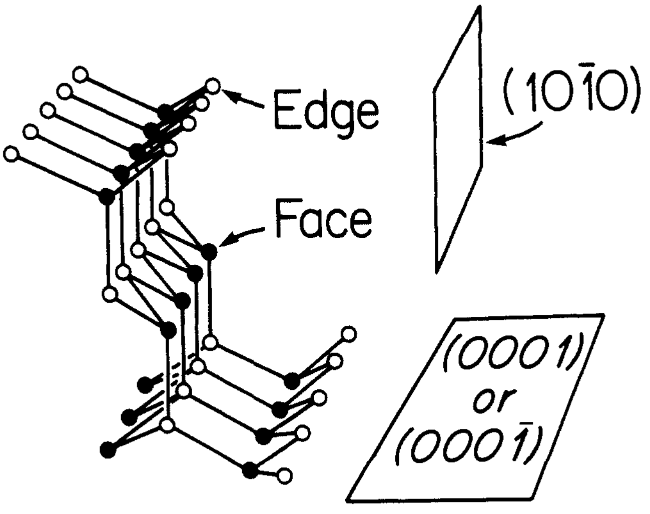

Figure 4. Step on (0001) and (000$\bar{1}$) ZnO surfaces.

When H^- binds to a Zn^{2+} site its strongest σ interactions are with the empty Zn surface state orbitals and the filled Zn 4s and 3d surface state orbitals. The lowest orbital with substantial hydrogen 1s character is bonding to Zn $3d_{z^2}$ and contains 0.48 electron. The next orbital contains 0.13 electron and is antibonding to Zn $3d_{z^2}$ and bonding to Zn 4s; the net result is an orbital with mostly nonbonding character. The next two orbitals have 0.10 and 0.20 electron on the hydrogen and are donation bonds to the empty Zn 4s + 4p surface state with some antibonding Zn 3d and 4s character mixing in. These charges on H add up to 0.91 electron, and the net charge of H^- is −0.22. The difference, 0.31, is due to many small contributions to the density on H^- from throughout the filled bands. The back donation from H^- to the empty surface state is largely responsible for the 0.78 electron reduction in the −1 charge of H^-. The surface state actually adds one more orbital within the filled band region, and this takes the two electrons from the orbitals which are the antibonding counterparts to the Zn–H d–s σ bond. This orbital is indicated by the upward-pointing arrow from the H 1s level and is off the scale of the figure. If there were no surface states the interaction would be closed shell and H^- would not chemisorb. This is born out when we examine H^- adsorption to second layer Zn^{2+} sites and find no binding.

When H• binds to Zn^{2+} the structure and orbital interactions are the same as for H^-, as even is the charge, −0.22 electron, on the chemisorbed H. In this case there is a hole at the top of the O 2p band. Because of the charge transfer to H, the adsorption energy is 0.48 eV stronger than that of H^-.

The correlation diagram for H^+ bonding to O^{2-} is shown in Figure 3. The lowest orbital has a bonding overlap between the H 1s orbital and an O 2s orbital; 0.25 electron resides on H. The next orbital is bonding to Zn 3d band orbitals because these orbitals are the bonding counterparts of the O 2p–Zn 3d interaction, so they have amplitude on the oxygens. There is 0.10 electron in this orbital. The next orbital has 0.12 electron on H and is bonding to the Zn 4s band surface oxygen components. For both of the previously mentioned orbitals the O 2p band hybridizes in some. The top orbital correlates with O 2p band surface states and has 0.05 electron on H. The antibonding counterpart σ* orbital lies very high and is, of course, empty. The charges on H add up to 0.52 electron, meaning a net atomic charge of +0.48. The actual net charge is only +0.29 because of several weaker σ bonding interactions throughout the filled bands; these are not shown.

Clearly, when two H$^•$ adsorb to Zn^{2+} and a neighboring O^{2-} the results are Zn^{2+}–H$^-$ and O^{2-}–H$^+$ and the highest filled level is at the top of the O 2p band. The binding energy is maximum. If both H$^•$ went on Zn^{2+} sites to make 2 Zn^{2+}–H$^•$, the highest filled level would still be at the top of the O 2p band, but the binding energy is weakest (assuming corrections) because 2 Zn^{2+}–H$^•$ bonds are weaker than 1 Zn^{2+}–H$^-$ and 1 O^{2-}–H$^+$ bonds, the latter of these being relatively very strong. If both H$^•$ bind to O^{2-} to give 2 O^{2-}–H$^+$ + 2e$^-$, the two electrons must go into high-lying empty surface state orbitals and the total binding energy is intermediate in magnitude (assuming corrections). If edge states were available due to surface restructuring, the adsorption energy would increase but would still be weaker than heterolytic binding.

From the above it is clear that H_2 will adsorb heterolytically as Zn^{2+}–H$^-$ + O^{2-}–H$^+$ because of energy reasons (this is the most stable state) and because of configurational reasons (heterolytic Zn^{2+} and O^{2-} sites are adjacent and can participate in activating H_2, while homolytic Zn^{2+} and O^{2-} sites are widely separated and therefore provide no mechanism for dissociating H_2).

Heterolytic Coverage

It was mentioned in the introduction to this study that only 5–10% of the surface of ZnO powders are observed to heterolytically adsorb H_2. We see that if the surfaces of the powder grains were all of the $(10\bar{1}0)$ crystallographic orientation 100% of the sites would be involved, so clearly the grains present other crystallographic orientation in addition to or in place of $(10\bar{1}0)$ surfaces. We do not know the actual morphology, but it is interesting to note that even (0001) (Zn^{2+}) and $(000\bar{1})$ (O^{2-}) surfaces may also adsorb H_2 heterolytically because they are covered by step defects.[14] These have double layer step heights as shown in Figure 4. On the (0001) surface there is one row of Zn^{2+} edge sites, and there is one row of O^{2-} surface sites on the step face. To maintain stoichiometry and charge balance there will be compensating defects on another surface. If on the opposite side of the crystal there is a $(000\bar{1})$ surface, then it will have one step for every step on the (0001) surface. Each step will have an edge row of O^{2-} sites and a row of Zn^{2+} surface sites on the step face. The steps on both the (0001) and $(000\bar{1})$ surfaces will be capable of adsorbing H_2 heterolytically, but because the heterolytic Zn^{2+} and O^{2-} sites are not adjacent, such adsorption will be kinetically retarded, and neither will be stabilized as strongly by the electrostatic coupling of the Zn^{2+}H$^-$ and O^{2-}H$^+$ dipoles.

Hydrogen Atom Adsorption and Surface Conductivity

The following is speculative, but plausible. We hope it will stimulate further work.

As discussed earlier, heterolytic adsorption of H_2 does not increase the conductivity of ZnO, and from the electronic structure discussion it is clear this is because no electrons are promoted to the surface conduction band. Hydrogen atom adsorption on the $(000\bar{1})$ surface increases the surface conductivity rapidly, yet on the smooth surface there are no empty Zn 4s + 4p surface states. Since the surface is stepped, though the concentration of steps does not seem to be known, it is probable that H$^•$ will adsorb preferentially and rapidly at O^{2-} edge sites, filling the Zn^{2+} step face surface state conduction band. The bulk conduction band bottom lies high in our calculations, at around −4 eV, but the optical band gap of 3.3 eV would place it at −7.3 eV, in the region of our present Zn^{2+} surface state band, which itself may lie a few tenths of an electronvolt too high. Thus most H$^•$ is likely to be found initially at edge sites where it can reduce the low-lying Zn^{2+} surface states. The reduced coordination of edge O^{2-} may contribute to an increased H$^•$ bonding strength as in the case of MgO.[12] Conductivity may increase relatively rapidly as the projecting and accessible edge O^{2+} sites are saturated by H$^•$. Why the conductivity does not decrease after a long time when H$^•$ will be expected to saturate the reduced step face Zn$^+$ sites is not clear. Perhaps the nonadjacency of the Zn^{2+} and O^{2-} heterolytic pair sites makes them less stable. Perhaps there is further relaxation which destabilizes H$^•$ bonding at these sites. Perhaps the final conductivity is governed by the bulk, though evidence given below makes this an unlikely explanation.

H$^•$ adsorption on the (0001) surface increases the surface conductivity slowly and this may be because the step face O^{2-} sites are slow to fill due to their relatively hidden location. As they fill, Zn^{2+} edge surface conduction band states will become occupied and conductivity will increase. When all edge face O^{2-} have H$^•$ bonded to them, the lower edge state conduction band is filled and so conduction will be through the surface state conduction band possibly involving the upper edge band or step base zinc surface states. These sites may be free of hydrogen because of heterolytic H_2 desorption. If step concentrations on (0001) and $(000\bar{1})$ surfaces are the same, the final surface state conductivities will be the same, as observed for polar surfaces formed by cleavage of a single crystal.[14] In fact, the concentration of H$^•$ is at least 10^{13} per cm^2, and the electron concentration is about 10^{13} per cm^2 on both surfaces.[14] On an ideal unreconstructed (0001) surface there are 4.1×10^{15} O^{2-} sites per cm.^{2} This suggests a concentration of step edge and face atoms of about 1 in 400 surface atoms if ZnO conduction by electrons in the bulk conduction band is excluded.

There is an additional experimental result which our model for H$^•$ adsorption and the resulting surface conductivity on stepped (0001) and $(000\bar{1})$ surfaces explains. When oxygen is added, the conductivity of the (0001) surface decreases more rapidly than that for the $(000\bar{1})$ surface.[14] This is expected for the same reason H$^•$ increases the conductivity of the O^{2-} covered $(000\bar{1})$ surface more rapidly. Oxygen will oxidize the reduced zinc conduction band sites. On the Zn^{2+} covered (0001) surface the reduced zinc step edge sites are more readily accessible to oxygen than in the case of the $(000\bar{1})$ surface, where the reduced zinc is on the step face.

Conclusions

We have explained the electronic factor behind heterolytic adsorption of H_2 on Zn $(10\bar{1}0)$. Such adsorption allows a strong O:H and a fairly strong Zn:H bond to form. Homolytic adsorption on zinc results in two weak Zn·H bonds and homolytic adsorption on oxygen requires the high energy promotion of two electrons to zinc surface or bulk conduction band states. This explanation will also apply to other oxides with empty metal valence bands, including alkaline earth oxides discussed in ref 12. Similar reasoning applies to CH activation as shown in other work from this laboratory.[15,16] The photoactivation processes discussed in ref 15 may also be important to H_2 activation on some oxide surfaces.

Our second finding is a rationalization of the conductivities of stepped (0001) and $(000\bar{1})$ surfaces which are induced by H$^•$ adsorption. Further experimental studies of these stepped surface would be worthwhile. The weakened intensity of the CO 4σ photoemission signal for CO adsorbed on the $(000\bar{1})$ surface has been attributed to the low concentration of step face Zn^{2+} adsorption sites. There is, however, another viewpoint regarding restructuring on the (0001) and $(000\bar{1})$ surfaces. In this view one-fourth of the cations and anions are missing from the (0001) and $(000\bar{1})$ surfaces, respectively. This suggestion, which is based on a Madelung energy analysis,[17] implies that a (2×2) surface should form. Despite the fact this was not observed,[17,18] (2×2) restructuring of the (0001) surface has been used as a basis for rationalizing the coverage dependence of H_2 and CO adsorption on ZnO pressed powders.[19] Such forms of ZnO should have high concentrations of step and edge sites and $(10\bar{1}0)$ and other crystal

---

[14] Henzler, M. *Surf. Sci.* **1973**, *36*, 109.

[15] Anderson, A. B.; Ray, N. K. *J. Am. Chem. Soc.* **1985**, *107*, 253.

[16] Mehandru, S. P.; Anderson, A. B.; Brazdil, J. F.; Grasselli, R. K., submitted for publication.

[17] Nosker, R. W.; Mark, P.; Delevine, J. *Surf. Sci.* **1970**, *19*, 291.

[18] Campbell, B. D.; Hague, C. A.; Farnsworth, H. E. *Proceeding of the Fourth International Materials Symposium*; Somorjai, G. A., Ed.; Wiley: New York, 1969.

[19] Griffin, G. L.; Yates, J. T., Jr. *J. Chem. Phys.* **1982**, *77*, 3744, 3751.

facets present, and it would be worthwhile to consider the data obtained in ref 19 in terms of them.

Acknowledgment is made to the donors of the Petroleum Research fund, administered by the American Chemical Society, for support of this research through a Summer Research Fellowship for J.A.N. A.B.A. owes W. Keith Hall thanks for many stimulating discussions.

Registry No. ZnO, 1314-13-2; H, 12385-13-6; H_2, 1333-74-0.

Bonding in Transition-Metal Methylene Complexes. 3. Comparison of Cr and Ru Carbenes; Prediction of Stable $L_nM(CXY)$ Systems[1]

Emily A. Carter[†] **and William A. Goddard III***

Contribution No. 7336 from the Arthur Amos Noyes Laboratory of Chemical Physics, California Institute of Technology, Pasadena, California 91125. *Received December 9, 1985*

Abstract: The electronic structure of the lowest carbene state of a representative early-transition-metal complex, $CrCH_2^+$ ($^6A_1$ symmetry), has been examined by using ab initio techniques. Its properties reveal a complex with a single σ-donor bond from singlet CH_2 to high-spin (d^5) Cr^+ and no π-back-bond, resulting in a low bond energy (38.7 kcal/mol) and a large carbene–alkylidene state splitting (18.8 kcal/mol). These results are contrasted with Ru carbene (possessing both σ- and π-donor bonds) properties [D_e(Ru=C) = 65.8 kcal/mol and ΔE(carbene–alkylidene) = 12.9 kcal/mol]. This comparison enables, for the first time, a separation of σ-donor bond strengths from π-donor bond strengths. Finally, using only valence electron properties, we are able to predict stabilities of $L_nM(CXY)$ complexes (e.g., how substituents at carbon affect the preference for bridging vs. terminal CXY), discussing trends for the entire transition series.

I. Introduction

Terminal metal carbene and alkylidene complexes are ubiquitous throughout the transition elements.[2] The nomenclatural distinction between "carbene" and "alkylidene" represents a fundamental difference in reactivity.[3] Metal carbene complexes usually behave as electrophiles, with typical reactions including Lewis base adduct formation via attack at the carbon center[4]

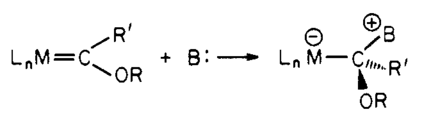
(1)

and stoichiometric cyclopropanation of olefins[5]

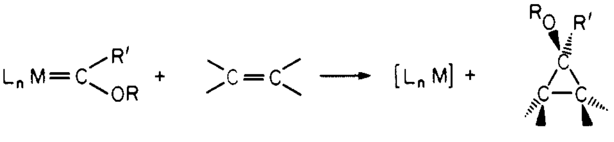
(2)

On the other hand, metal alkylidene complexes are nucleophilic, undergoing Wittig-type alkylations,[6,7] Lewis acid adduct formation,[8]

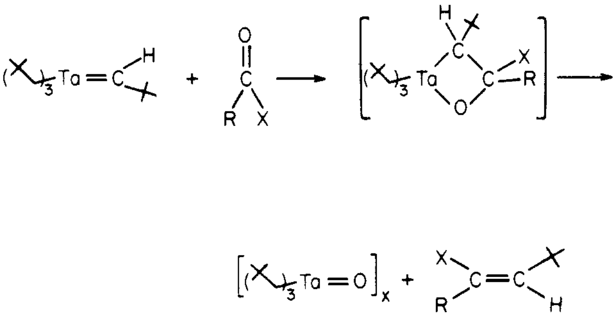
(3)

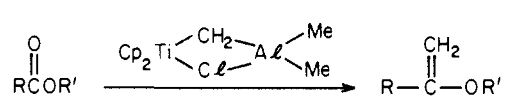
(4)

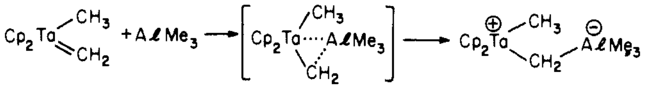
(5)

and olefin metathesis.[9]

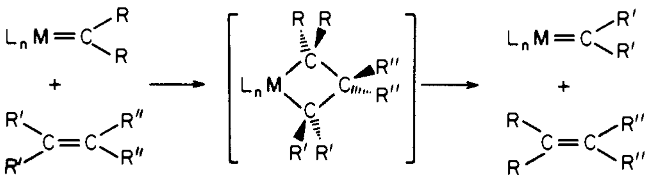
(6)

These two greatly different modes of reactivity reflect a dra-

---

[†] National Science Foundation Predoctoral Fellow, 1982–1985.

(1) (a) Paper 1 of this series: Carter, E. A.; Goddard, W. A., III *J. Phys. Chem.* **1984**, *88*, 1485. (b) Paper 2: Carter, E. A.; Goddard, W. A., III *J. Am. Chem. Soc.* **1986**, *108*, 2180. (c) Earlier work on high-valent alkylidene complexes includes: Rappé, A. K.; Goddard W. A., III *J. Am. Chem. Soc.* **1982**, *104*, 297; **1982**, *104*, 448; **1980**, *102*, 5114.

(2) For a comprehensive review, see: Dötz, K. H.; Fischer, H.; Hofmann, P.; Kreissl, F. R.; Schubert, U.; Weiss, K. *Transition Metal Carbene Complexes*; Verlag Chemie: Deerfield Beach, FL, 1984.

(3) Collman, J. P.; Hegedus, L. S. *Principles and Applications of Organotransition Metal Chemistry*; University Science Books: Mill Valley, Ca, 1980; Chapter 3.

(4) (a) Wong, W.-K.; Tam, W.; Gladysz, J. A. *J. Am. Chem. Soc.* **1979**, *101*, 5440. (b) Yu, Y. S.; Angelici, R. J. *Organometallics* **1983**, *2*, 1018. (c) Kuo, G.-H.; Helquist, P.; Kerber, R. C. *Ibid.* **1984**, *3*, 806.

(5) (a) Fischer, E. O.; Dötz, K. H. *Chem. Ber.* **1970**, *103*, 1273. (b) Dötz, K. H.; Fischer, E. O. *Ibid.* **1972**, *105*, 1356. (c) Stevens, A. E.; Beauchamp, J. L. *J. Am. Chem. Soc.* **1979**, *101*, 6449. (d) Brandt, S.; Helquist, P. J. *Ibid.* **1979**, *101*, 6473. (e) Brookhart, M.; Humphrey, M. B.; Kratzer, H. J.; Nelson, G. O. *Ibid.* **1980**, *102*, 7803. (f) Brookhart, M.; Tucker, J. R.; Husk, G. R. *Ibid.* **1981**, *103*, 979. (g) Casey, C. P.; Vollendorf, N. W.; Haller, K. J. *Ibid.* **1984**, *106*, 3754. (h) Casey, C. P.; Shusterman, A. J. *Organometallics* **1985**, *4*, 736. (i) Brookhart, M.; Studabaker, W. B.; Husk, G. R. *Ibid.* **1985**, *4*, 943. (j) Casey, C. P.; Miles, W. H.; Tukada, H. *J. Am. Chem. Soc.* **1985**, *107*, 2924. (k) Stevens, A. E.; Beauchamp, J. L. *Ibid.* **1978**, *100*, 2584.

(6) Schrock, R. R. *J. Am. Chem. Soc.* **1976**, *98*, 5399.

(7) (a) Tebbe, F. N.; Parshall, G. W.; Reddy, G. S. *J. Am. Chem. Soc.* **1978**, *100*, 3611. (b) Pine, S. H.; Zahler, R.; Evans, D. A.; Grubbs, R. H. *Ibid.* **1980**, *102*, 3270.

(8) Schrock, R. R. *J. Am. Chem. Soc.* **1975**, *97*, 6577.

0002-7863/86/1508-4746$01.50/0 © 1986 American Chemical Society